ChemComm

ROYAL SOCIETY OF CHEMISTRY

COMMUNICATION

View Article Online
View Journal | View Issue



Cite this: *Chem. Commun.*, 2023, 59, 4320

Received 2nd February 2023,
Accepted 8th March 2023

DOI: 10.1039/d3cc00474k

rsc.li/chemcomm



# Aggregated coordination polymers of $Ag^+$ with a cysteine derivative ligand containing an AIEgen†

Jing-Jing Quan, Qian Wang, Zhao Li and Yun-Bao Jiang *

**We investigated coordination polymers of $Ag^+$ with a cysteine-based thiol ligand designed to contain a tetraphenylethylene AIEgen (L- and D-1). The coordination polymers, forming in a variety of protic and aprotic organic solvents, such as THF, $CH_3CN$ and $CH_3OH$, were shown to undergo aggregation in $H_2O$/THF binary solvents at water volume fractions above 50%, where emission was substantially enhanced while the CD profile was reversed, yet the dependence of the CD signal on ee remained S-shaped for the polymers in the aprotic organic solvents THF and $CH_3CN$, in contrast to that in protic solvents $CH_3OH$ and $C_2H_5OH$.**

We have recently shown that the coordination polymers of $Ag^+$ with chiral thiol ligands exhibit interesting properties,[1–10] including overall supramolecular chirality with respect to the molecular and supramolecular chirality of the ligands,[6] properties consistent with their serving as functional materials for sensing,[1–4,8–10] and their being amenable to having their morphologies controlled.[7] We therefore considered extending these efforts to the study of aggregates of these coordination polymers, a subject not yet pursued despite the wealth of investigations on the aggregates of the covalent polymers. In this regard, it was critical to design a thiol ligand whose properties would be sensitive to the existing forms of the polymers. We thus considered a cysteine-based chiral ligand containing an AIEgen whose emission has been shown to be sensitive to the extent of aggregation.[5,11,12] In the current work, we investigated coordination polymers of $Ag^+$ with L- and D-**1** forms of a chiral ligand (Scheme 1) in organic solvents and the aggregates of these polymers in water-rich tetrahydrofuran (THF) solutions, and investigated their substantially differing properties, and intriguing chirality.

We previously showed the coordination polymers of $Ag^+$ with cysteine in aqueous solutions to be stabilized by both the $Ag^+\cdots Ag^+$ interactions (the argentophilic interactions)[13–15] along the polymeric backbone and by electrostatic interactions between the ligands attached to the backbone.[2,10] The interaction network has been assumed to be responsible for allowing the molecular chirality of the ligand to be transferred into the polymeric backbone as a supramolecular chirality—with this assumption based on, for example, 350 nm-wavelength CD signals of the chromophores related to the argentophilic interactions in the $Ag^+$ cysteine coordination polymers in aqueous solutions.[2] This feature has allowed for a variety of photofunctional applications, such as spectral sensing, *via* tuning the interactions between ligands on the polymeric backbone.[1–4,8–10] In those investigations, the coordination polymers were made to behave as individual polymeric species. We therefore proposed to investigate the behavior of the coordination polymers in their aggregated forms, a subject not much pursued. For this purpose, we designed a cysteine-based ligand (L-/D-**1**, Scheme 1) by introducing an AIEgen, namely tetraphenylethylene (TPE), whose emission was expected to be sensitive to the extent of aggregation. A control compound, namely L-**2** bearing an AIEgen directly linked to the cysteine residue[5] and having only three instead of four phenyl spacers, was employed (Scheme 1). Syntheses of these ligands are described in the ESI† (Schemes S1 and S2). The new compounds were fully characterized by performing $^1H$ and $^{13}C$ NMR and mass spectrometry (MS) experiments (Fig. S36–S44, ESI†) and the $Ag^+$–L-**1** coordination polymers were characterized using MALDI-TOF MS (Fig. S45, ESI†).

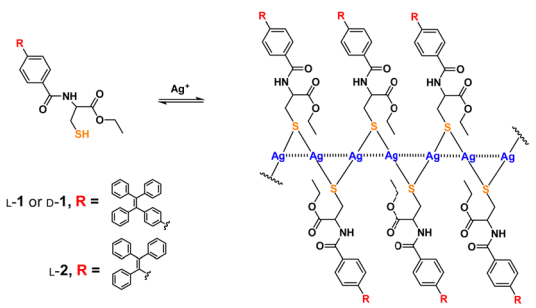


Scheme 1 Formation of coordination polymers of $Ag^+$ with thiol ligand **1** and its control compound **2**. Dashed lines through the backbone represent $Ag^+\cdots Ag^+$ interactions.[16]

*Department of Chemistry, College of Chemistry and Chemical Engineering, The MOE Key Laboratory of Spectrochemical Analysis and Instrumentation, and iChEM, Xiamen University, Xiamen 361005, China. E-mail: ybjiang@xmu.edu.cn*

† Electronic supplementary information (ESI) available. See DOI: https://doi.org/10.1039/d3cc00474k

Absorption and CD spectra of D-**1** in the presence of increasing concentrations of $Ag^+$ were first examined for the compound in THF (Fig. 1a). D-**1** by itself exhibited an absorption at 325 nm; this absorption red-shifted, specifically to 340 nm, when $Ag^+$ cation was introduced, suggesting the occurrence of the $Ag^+\cdots Ag^+$ interactions.[16–18] Meanwhile, negative and positive CD signals appeared at 350 nm and 295 nm, respectively. The CD profile of L-**1** in the presence of $Ag^+$ in THF was found to be the mirror image of that of D-**1** with $Ag^+$, confirming that the chirality of the formed species originated from the molecular chirality of ligand L-**1** or D-**1**.[19–21] Plots of the absorbance or CD signals against concentration of $Ag^+$ (Fig. S1, ESI†) suggested a 1 : 1 stoichiometry, agreeing with that deduced from the Job plots (Fig. S2, ESI†). DLS results (Fig. S3, ESI†) and TEM (Fig. S4, ESI†), SEM and AFM images (Fig. 2) indicated the formation of helical fiber structures with diameters of *ca.* 28 nm and lengths of up to tens of micrometers, *i.e.*, the coordination polymers of $Ag^+$ with L-**1** or D-**1** (Scheme 1). The helical senses of the $Ag^+$–L-**1** and $Ag^+$–D-**1** coordination polymers formed in THF were left- (*M*) and right-handed (*P*), respectively (Fig. 2a–d). The acquired $^1$H NMR spectrum of the ligand in THF-*d*8 showed well-resolved signals (Fig. S5, ESI†), which increasingly broadened and became less well-resolved when increasing concentrations of $Ag^+$ were added, evident for the formation of the coordination polymers.[22] The efficient communication of the molecular chirality of the ligand into the chromophore relating to the $Ag^+\cdots Ag^+$ interactions along the polymeric backbone thus suggested the occurrence of interactions between ligands and their networking with the $Ag^+\cdots Ag^+$ interactions.[2,4–6,9] Fluorescence of D-**1** in THF was observed at 490 nm upon excitation at 350 nm, and was increasingly enhanced when increasing amounts of $Ag^+$ were added up to 1 equivalent of $Ag^+$, at which point the fluorescence enhancement finally levelled off ($I_{max}/I_0$) at 2.3 (Fig. S6, ESI†). Absorption and CD spectra recorded next of the coordination polymers in a variety of solvents (Fig. 1b) showed profiles similar to those in THF, except for an extremely weak CD signal in water. We thus tentatively concluded that the coordination polymers formed in all the tested solvents, despite no crystal structures obtained of the coordination polymers even after many trials. The $Ag^+$-thiolate coordination polymers may have formed intertwined polymeric structures (see ref. 19 and 23).

To exclude the effect of self-aggregation of the coordination polymers due to stacking of the large aromatic TPE moieties, various concentrations were tested. As illustrated in Fig. S7–S10 (ESI†), addition of $Ag^+$ to THF solutions of **1** at low concentrations (5 and 15 μM) led to spectral changes similar to those observed at the higher concentration of 25 μM. Furthermore, the experiments with coordination polymers at the different concentrations all showed nearly the same maximum fluorescence enhancement, $I_{max}/I_0$, of 2.3.

These measurements thus confirmed that it was the $Ag^+\cdots Ag^+$ interactions that induced the assembly of L-**1** or D-**1** in the presence of $Ag^+$.

Hydrophobic TPE derivatives have been shown to undergo aggregation in water-rich solutions.[24–26] However, D-**1** at 25 μM was found to be CD silent in $H_2O$/THF mixtures of various compositions (Fig. S11, ESI†), indicating that D-**1** at 25 μM existed in a monomeric form. In contrast, $Ag^+$–D-**1** and $Ag^+$–L-**1** coordination polymers at the same ligand concentration of 25 μM were observed to be CD active—and, more interestingly, signs of the Cotton effects related to the ligand-to-metal–metal charge transfer (LMMCT) at 350 nm and *N*-benzamide moiety at 272 nm were found inverted when the volume content of $H_2O$ reached 50% (Fig. 3a and b). Meanwhile, hypochromatic shifts by *ca.* 10 nm, specifically from 272 nm to 260 nm and 350 nm to 340 nm, were observed together with a remarkable reduction in the CD intensity, compared to those in pure THF (Fig. 3 and Fig. S12a, ESI†). Compared to the CD curves of $Ag^+$–L-**1**, those of $Ag^+$–D-**1** showed a reversed, mirror image relationship (Fig. 3b and Fig. S12b, ESI†). In both cases, the CD profiles remained unchanged for solvent composition VTHF/V$H_2O$ values varying from 10 : 0 to 6 : 4, but then the signal was weakened and then reversed sign as the volume ratio was further changed to 5 : 5 and then 4 : 6, respectively. Similar observations were made at the same volume composition of 5 : 5 in solutions with a lower concentration of the coordination polymers (15 μM, Fig. S13 and S14, ESI†).

SEM images indicated that with increasing water volume fraction, the helical polymeric structure of the $Ag^+$–D-**1** coordination polymers formed in pure THF gradually transformed into nanoparticles in the water-rich solutions (Fig. S15, ESI†). A plot of DLS-derived hydrodynamic diameter *versus* water volume fraction showed a "bell" shape, with a plateau between water volume fractions of 20% and 70% (Fig. S16, ESI†). Fluorescence spectra of L-**1** in $H_2O$/THF binary mixtures in the absence (Fig. 4a) and presence of $Ag^+$ (Fig. 4b) suggested that the $Ag^+$–L-**1** coordination polymers aggregated in $H_2O$/THF volume compositions higher than 5 : 5, while L-**1** itself aggregated at a much higher water volume fraction of 70% (Fig. 3c and d), following a model of the aggregation-induced emission (AIE).[11,12,27–29] This result indicated that the formation of coordination polymers of the thiol ligand promoted the aggregation. The observation of the inversion of the CD profile of the coordination polymers at the solvent composition at which aggregation occurred suggested that it was the aggregation of the coordination polymers that led to the inversion of the supramolecular chirality. Also note that the aggregation of the coordination polymers in water-rich $H_2O$/THF solutions resulted in relatively high enhancements of the emission, specifically $I/I_0 > 3$ (Fig. 3c, d and 4 *versus* Fig. S6, ESI†). A similar CD profile inversion was not observed in the same series of $H_2O$/THF solutions of the coordination polymers of $Ag^+$ with the control ligand L-**2**, *i.e.*, that with three instead of four phenyl groups ($Ag^+$–L-**2**, Fig. S17, ESI†). The signals of the fluorescence spectra of the $Ag^+$–L-**2** coordination

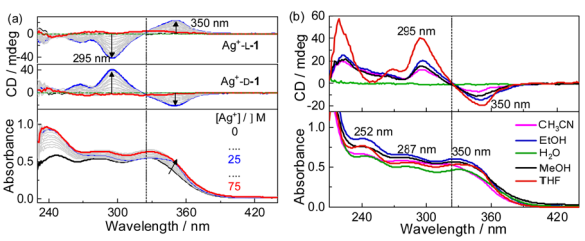


Fig. 1 (a) Absorption (bottom panel) and CD (top panel) spectra of D-**1** in the presence of increasing concentrations $Ag^+$ in THF and (b) absorption and CD spectra of $Ag^+$–D-**1** coordination polymers in indicated solvents. Dissymmetry factor $|g_{abs}|$ values of the coordination polymers in THF were calculated from (a), and found to be $3.39 \times 10^{-3}$ at 295 nm and $1.22 \times 10^{-3}$ at 350 nm. [L-**1**] = [D-**1**] = 25 μM, [$Ag^+$] = 0–75 μM (in panel a) or 25 μM (in panel b).

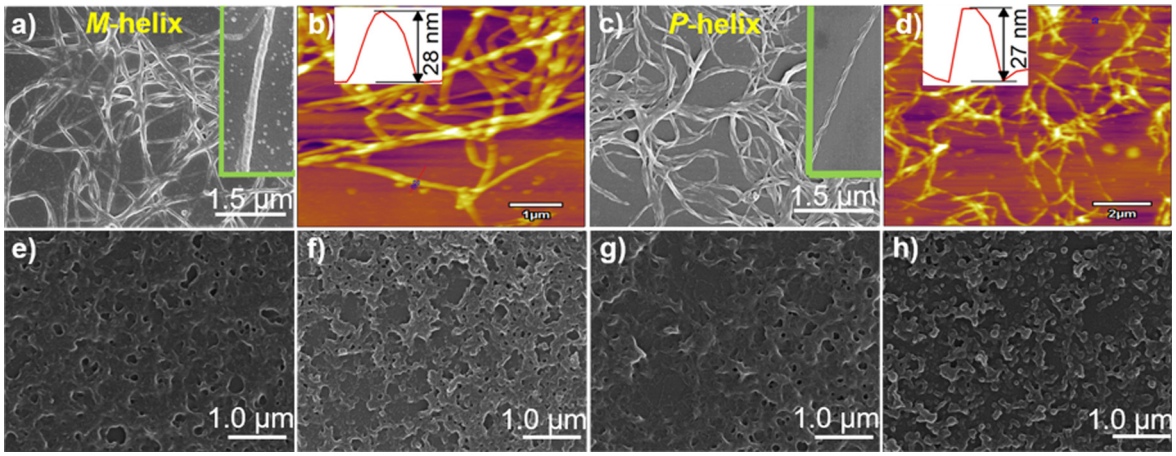


Fig. 2 SEM and AFM images of supramolecular structures of (a and b) $Ag^+$–L-**1** formed in THF, and (c–h) $Ag^+$–D-**1** in (c and d) THF, (e) EtOH, (f) MeOH, (g) $CH_3CN$ and (h) $H_2O$. The insets in (a) and (c) show, respectively, two types of polymeric structures, namely the *M*-helix of $Ag^+$–L-**1** and *P*-helix of $Ag^+$–D-**1**. [$Ag^+$–L-**1**] = [$Ag^+$–D-**1**] = 25 μM.

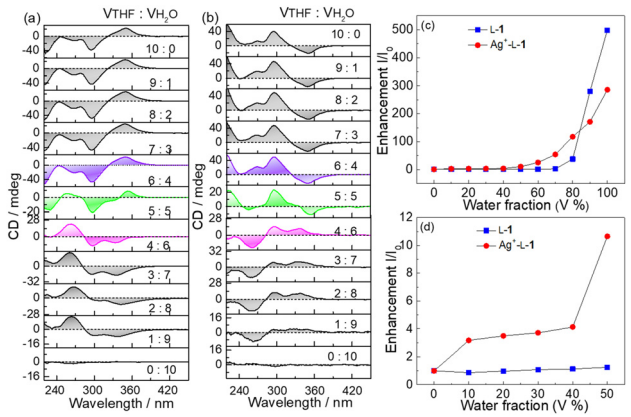


Fig. 3 (a and b) CD spectra of (a) $Ag^+$–L-**1** and (b) $Ag^+$–D-**1** in THF containing increasing volume fractions of water. (c and d) Plots of the enhancements of fluorescence of L-**1** and $Ag^+$–L-**1** at 484 nm *versus* water volume fraction. $\lambda_{ex}$ = 350 nm, [$Ag^+$] = [L-**1**] = [D-**1**] = 25 μM.

polymers did not undergo a dramatic enhancement when in the water-rich solvents, *i.e.*, up to 80% by volume of $H_2O$ (Fig. S18–S20, ESI†). The difference in aggregation between the coordination polymers of $Ag^+$ with **1** and **2** indicated a contribution of the additional benzene spacer in **1** to increasing the flexibility of the TPE AIEgen so that its emission could be more sensitive to the occurrence of aggregation, in addition to its contribution to increasing the hydrophobicity of ligand **1**. This feature is expected

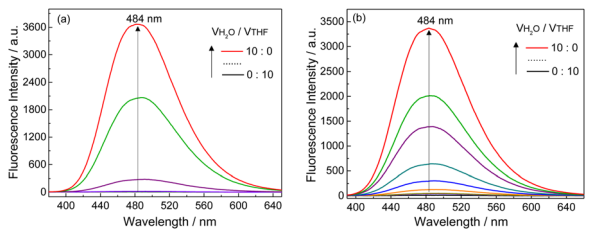


Fig. 4 Fluorescence spectra of (a) L-**1** and (b) $Ag^+$–L-**1** in $H_2O$/THF mixtures with increasing volume fractions of $H_2O$. $\lambda_{ex}$ = 350 nm, [L-**1**] = [$Ag^+$–L-**1**] = 25 μM.

to be important for future applications in developing photofunctional materials in terms of ligand structure design. For this purpose, pH and temperature effects on the $Ag^+$–D-**1** or $Ag^+$–L-**1** coordination polymers in THF and/or 3 : 7 (v/v) THF/$H_2O$ by using their CD and emission spectral variations were examined. As shown in Fig. S21–S23 (ESI†), the chiroptical activity of $Ag^+$–D-**1** coordination polymers did not change much as the pH was changed in the range 3.6–9.0 while the emission intensity was slightly quenched; at higher pH, precipitations started to occur. We concluded there to be a negligible influence of pH in the 3.6–9.0 range on the stability of coordination polymers in 3 : 7 (v/v) THF/$H_2O$. Moreover, effect of temperature on CD and fluorescence of coordination polymers in THF and 3 : 7 (v/v) THF/$H_2O$ binary mixtures were investigated. Upon increasing the solution temperature from 20 °C to 60 °C, the intensities of the CD signals of $Ag^+$–L-**1** coordination polymers in THF slightly decreased (Fig. S24 and S25, ESI†), suggesting a gradual disassembly of the coordination polymers. When the temperature was then lowered back to 20 °C, the original CD signals were nearly fully restored. The fluorescence also displayed a reversible change with change in temperature (Fig. S26 and S27, ESI†), both suggesting an excellent thermostability of the $Ag^+$–L-**1** coordination polymers within the tested temperature range. In 3 : 7 (v/v) THF/$H_2O$, however, an irreversible CD change was observed (Fig. S28 and S29, ESI†), and the emission intensity of the coordination polymers failed to recover to the original value after a cycle of heating and cooling (Fig. S30 and S31, ESI†), indicating a poorer stability of the aggregates of the coordination polymers when in water-rich THF solutions.

The supramolecular chirality of the coordination polymers was further probed by examining their CD profiles as a function of the enantiomeric excess (ee) of the ligand.[30] In aprotic organic solvents, namely THF (Fig. 5a and b and Fig. S32, ESI†) and $CH_3CN$ (Fig. 5c and d and Fig. S33, ESI†), the CD spectrum of the coordination polymers of $Ag^+$ formed with mixtures of the enantiomer pair L-**1** and D-**1** exhibited an "S"- or "Z"-shaped dependence on the ee of ligand, whereas an *anti*-"S"- or *anti*-"Z"-shaped dependence was observed in protic solvents, namely $CH_3OH$ (Fig. 5c and d and Fig. S34, ESI†) and

 

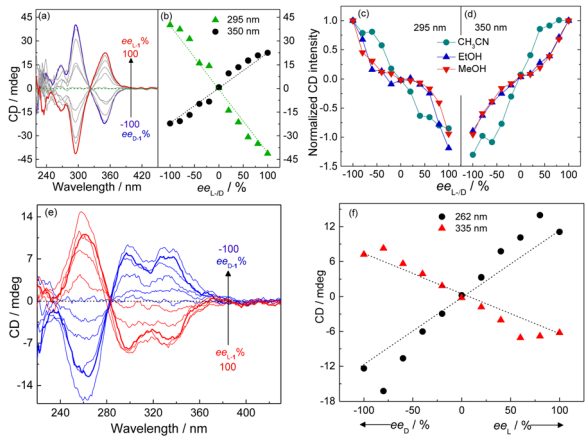


Fig. 5 (a and e) CD spectra and (b–d and f) plots of CD signals of $Ag^+$-**1** coordination polymers of varying ee of **1** in (a and b) THF, (e and f) 7 : 3 (v/v) $H_2O$/THF and (c and d) other protic ($CH_3OH$, $C_2H_5OH$) and aprotic ($CH_3CN$) organic solvents. [$Ag^+$] = 25 μM, [D-**1**] + [L-**1**] = 25 μM.

$C_2H_5OH$ (Fig. 5c and d and Fig. S35, ESI†). Interestingly, such dependence in water-rich 7 : 3 (v/v) $H_2O$/THF, in which the coordination polymers aggregated, was found to be "S"-shaped (Fig. 5e and f), despite the protic nature of the bulk solvent that would have led to an *anti*-"S"-shaped dependence as that observed for the individual coordination polymers in $CH_3OH$ or $C_2H_5OH$ (Fig. 5c and d and Fig. S34 and S35, ESI†). This result meant that the chromophores in the aggregated coordination polymers in water-rich protic solutions experienced a microenvironment similar to that in aprotic solvent.

In summary, we have reported coordination polymers of $Ag^+$ with a chiral cysteine-based ligand containing a TPE AIEgen. The formation of the coordination polymers in a variety of aprotic and protic organic solvents were indicated by spectral signals, *e.g.*, absorption, CD and emission signals, to exist in the form of individual polymeric species. In binary $H_2O$/THF solutions with water volume fractions above 50%, the coordination polymers were indicated to aggregate by morphology observations, a dramatic enhancement of the emission, characteristic of the AIE character of the TPE-fluorophore attached to the thiol ligand, and the inversion of the CD profile. Such behavior did not happen with the coordination polymers of the ligand with one phenyl group absent between the TPE-fluorophore and the cysteine residue, suggesting the importance of the structural design in which the ligand would more sensitively experience the extent of aggregation by extruding more into the bulk solution. An interesting observation made with the supramolecular chirality of the aggregated coordination polymers in the water-rich THF solution was that the CD-ee dependence remained S-shaped, opposite to that observed in protic solvents such as $CH_3OH$ and $C_2H_5OH$ in which the coordination polymers existed as individual polymeric species. This observation suggested a shielding of the chromophore of the coordination polymers in the aggregate forms from the protic solvent components. Our data thus showed that the aggregation of the dynamic coordination polymers resulted in substantial spectral changes, providing a new avenue to develop smart photofunctional materials by controlling the extent of aggregation of the coordination polymers. Creating a large variety of structural modifications on the thiol ligand would be expected to lead to many such opportunities, and with eventually tunable spectral properties.

This work has been supported by the National Natural Science Foundation of China (grant no. 21820102006, 91856118, 21904111 and 22241503) and the fundamental research funds for the central universities (grant no. 20720220005 and 20720220121).

## Conflicts of interest

There are no conflicts to declare.

## Notes and references

1 J.-S. Shen, D.-H. Li, Q.-G. Cai and Y.-B. Jiang, *J. Mater. Chem.*, 2009, **19**, 6219.
2 J.-S. Shen, D.-H. Li, M.-B. Zhang, J. Zhou, H. Zhang and Y.-B. Jiang, *Langmuir*, 2011, **27**, 481.
3 D.-H. Li, J.-S. Shen, N. Chen, Y.-B. Ruan and Y.-B. Jiang, *Chem. Commun.*, 2011, **47**, 5900.
4 Q. Zhang, Y. Hong, N. Chen, D.-D. Tao, Z. Li and Y.-B. Jiang, *Chem. Commun.*, 2015, **51**, 8017.
5 D.-D. Tao, Q. Wang, X.-S. Yan, N. Chen, Z. Li and Y.-B. Jiang, *Chem. Commun.*, 2017, **53**, 255.
6 Y. Yuan, Y.-W. Xiao, X.-S. Yan, S.-X. Wu, H. Luo, J.-B. Lin, Z. Li and Y.-B. Jiang, *Chem. Commun.*, 2019, **55**, 12849.
7 D.-D. Tao, J.-H. Wei, X.-S. Yan, Q. Wang, B.-H. Kou, N. Chen and Y.-B. Jiang, *Chem. Commun.*, 2020, **56**, 15133.
8 Q. Wang, S.-L. Dong, D.-D. Tao, Z. Li and Y.-B. Jiang, *Coord. Chem. Rev.*, 2021, **432**, 213717.
9 S.-L. Dong, Y. Xu, Y.-Z. Chen, X.-S. Yan, Z. Li, J.-W. Xie and Y.-B. Jiang, *Inorg. Chem.*, 2021, **60**, 5413.
10 Y. Xu, S.-L. Dong, X.-S. Yan, Q. Wang, Z. Li and Y.-B. Jiang, *Chem. Commun.*, 2021, **57**, 4311.
11 Y. N. Hong, J. W. Y. Lam and B. Z. Tang, *Chem. Commun.*, 2009, 4332.
12 Z. Zhao, H.-K. Zhang, J. W. Y. Lam and B. Z. Tang, *Angew. Chem., Int. Ed.*, 2020, **59**, 9888.
13 H. Schmidbaur and A. Schier, *Angew. Chem., Int. Ed.*, 2015, **54**, 746.
14 A. K. Jassal, *Inorg. Chem. Front.*, 2020, **7**, 3735.
15 O. Veselska, C. Dessal, S. Melizi, N. Guillou, D. Podbevsek, G. Ledoux, E. Elkaim, A. Fateeva and A. Demessence, *Inorg. Chem.*, 2019, **58**, 99.
16 C. Streb, C. Ritchie, D.-L. Long, P. Kögerler and L. Cronin, *Angew. Chem., Int. Ed.*, 2007, **46**, 7579.
17 C.-M. Che, M.-C. Tse, M. C. W. Chan, K.-K. Cheung, D. L. Phillips and K.-H. Leung, *J. Am. Chem. Soc.*, 2000, **122**, 2464.
18 Y. Akanuma, T. Imaoka, H. Sato and K. Yamamoto, *Angew. Chem., Int. Ed.*, 2021, **60**, 4551.
19 C. Li, K. Deng, Z. Tang and L. Jiang, *J. Am. Chem. Soc.*, 2010, **132**, 8202.
20 W. Jiang, Z.-b Qu, P. Kumar, D. Vecchio, Y. Wang, Y. Ma, J. H. Bahng, K. Bernardino, W. R. Gomes, F. M. Colombari, A. Lozada-Blanco, M. Veksler, E. Marino, A. Simon, C. Murray, S. R. Muniz, A. F. de Moura and N. A. Kotov, *Science*, 2020, **368**, 642.
21 M. Jakob, A. von Weber, A. Kartouzian and U. Heiz, *Phys. Chem. Chem. Phys.*, 2018, **20**, 20347.
22 H. Ju, Y. Tsuruoka, M. Hayano, E. Lee, K. M. Park, M. Ikeda, I. J. Ishi, S. Kuwahara and Y. Habata, *Angew. Chem., Int. Ed.*, 2021, **60**, 650.
23 B. O. Leung, F. Jalilehvand, V. Mah, M. Parvez and Q. Wu, *Inorg. Chem.*, 2013, **52**, 4593.
24 J. Li, J. Wang, H. Li, N. Song, D. Wang and B. Z. Tang, *Chem. Soc. Rev.*, 2020, **49**, 1144.
25 N. Lu, X. Gao, M. Pan, B. Zhao and J. Deng, *Macromolecules*, 2020, **53**, 8041.
26 Y. Wang, Y. Cai, L. Cao, M. Cen, Y. Chen, R. Zhang, T. Chen, H. Dai, L. Hu and Y. Yao, *Chem. Commun.*, 2019, **55**, 10132.
27 Y. Hong, J. W. Y. Lam and B. Z. Tang, *Chem. Soc. Rev.*, 2011, **40**, 5361.
28 Q. C. Peng, X. M. Luo, Y. J. Qin, T. Wang, B. Bai, X. L. Wei, K. Li and S. Q. Zang, *CCS Chem.*, 2022, **4**, 3686.
29 Y. J. Kong, Z. P. Yan, S. Li, H. F. Su, K. Li, Y. X. Zheng and S. Q. Zang, *Angew. Chem., Int. Ed.*, 2020, **59**, 5336.
30 X. Yan, Q. Wang, X.-X. Chen and Y.-B. Jiang, *Adv. Mater.*, 2020, **32**, 1904667.